



ATTACHMENT C
Marked Up New and Replacement Paragraphs and Claims

6/ Subst.
Spec.
G. S. only
6-20-02

A marked up copy of the replacement paragraphs and claims is provided as follows:

In the Disclosure

- Page 2, paras 004 and 005;*
- Page 7, paras 0018 and 0020;*
- Page 9, para 0035;*
- Page 10, paras 0045;*
- Page 11, para 0047;*
- Page 13, paras 0058 and 0060;*
- Page 16, delete para 0069;*
matrix A;
para 0070;
- Page 17, before para 0071, delete the three equations and insert Equations [2], [3] and [4];*
following paragraph 0071, delete matrixes S and R and insert new matrixes S
Equation [5] and R Equation [6];
- Page 18, para 0075;*
- Page 19, para 0077;*
delete matrix R and insert matrix Q Equation [7];
insert new para 0077.1;
- Page 22, para 0081;*
- Page 24, para 0088;*
- Page 26, para 0092;*
- Page 27, para 0096;*
- Page 28, Tables 2 and Table 3;*
- Page 29, para 00100;*
- Page 30, Table 4;*
para 00102;
- Page 31, Table 5;*

Page 32, Table 6;
Page 33, Tables 8 and 9;
Page 34, Tables 10, 11 and 12;
Page 35, para 00106;
Page 36, paras 00107, 00108, 00110 and 00112;
Page 37, para 00113;
Tables 13 and 14;
Page 38, para 00114;
Page 39, Equations [1], [2], [3], [4];
Page 40, Equations [5], [6] and [7];
para 00125;
Equations [8], [9], [10], [11] and [12];
Page 41, paras 00129 and 00131;
Page 43, paras 00134, 00135 and 00137;
Page 44, para 00138;
delete paras 139 through 142; and
Page 45, delete para 143.

In the Claims:

Claims 6, 13, 25, 33 and 38.

[004] It is therefore desirable to be able to precisely control the input components to obtain the desired target characteristic(s) with little waste. To obtain this control, a characteristic of the effluent of an industrial process should be precisely monitored in real time in order to provide feedback control on the amount of input [components] components, which should be added to the reactor to avoid under use or excessive use, and waste, of the input component.

[005] For example, in the pulp and paper industry, hydrogen peroxide and the hydroperoxy anion $[(HO_2^-)]$ (HO_2^-) are important input components for the oxidation and bleaching of wood pulps. In a typical pulp bleaching plant situation, the control of the bleaching chemicals is based on the brightness of the incoming pulp, the pulp flow, and the target brightness and pulp physical properties that are to be achieved. The factors of incoming pulp brightness, pulp flow, and target brightness are then used to calculate the amount of bleaching chemicals required to be added to the pulp to achieve a certain final target brightness. In another system, the brightness of the pulp is measured after bleaching chemicals are added and after allowing the reaction to occur for a defined reaction time. The resultant brightness value of the reaction is then measured and is used for feedback regulation of the bleaching chemicals.

[0018] In accordance with a further embodiment of the present invention there is provided an apparatus for determining a property of a sample comprising: a laser light source for irradiating at least a portion of the sample for generating a Raman emitted light from the sample; a detector for detecting the Raman emitted light from the sample, said detector for obtaining at least two measurements of [he] the Raman emitted light, a first measurement at a first wavenumber and a second measurement at a second wavenumber; and a processor for receiving and processing data from the detector for determining a non-linear relationship between the at least two measurements and the property of the sample.

[0020] [Further more,] Furthermore, in accordance with the invention there is provided a system for determining a property of a sample comprising: means for comparing at least two measurements including a first measurement at a first wavenumber and a second measurement at a second wavenumber, the at least two measurements corresponding to Raman emitted light between 200 cm^{-1} and 4000 cm^{-1} when the sample is irradiated with a laser; means for

determining a non-linear relationship between the at least two measurements and the property of the sample; and, means for determining the property of the sample in dependence upon the non-linear relationship.

[0035] Figure 13 [resents] presents the Raman spectra showing HOO^- and HOOH peaks at 850 cm^{-1} and $[877\text{ cm}^{-1},]$ 877 cm^{-1} , respectively;

[0045] Figure 24 shows Raman spectra of [Acetic] acetic acid and [Acetic] acetic acetate buffer solution. Top line: 0.05M acetic acetate buffer solution. Bottom line: 5% acetic acid solution (scaling X 0.2).

[0047] A sample of the effluent 6 is diverted to a Raman spectrometer 10 for the purpose of obtaining at least two Raman measurements of [UV light absorption of] the effluent 6 and then calculating the ratio of the two measurements. The ratio of the Raman emitted light intensity measurements have been found to correlate to various characteristics of the pulp effluent. For example, characteristics such as pulp brightness, pH, and pulp yellowness, and residual peroxide can be determined through the use of different Raman wavenumbers in the ratio.

[0058] 2. *Processing*. The processing of raw data to reduce noise and optimize the ability of the chemometric techniques to compare known spectra with unknown spectra or to act on specific features for the spectra of a multi-components solution to permit analysis of multi-components solutions or to adjust for noise or drift. The following preprocessing steps were explicitly identified: a) noise reduction or smoothing; b) Fourier or Walsh transformations; c) first or second derivatives; and [d)correction] d) correction for drift.

[0060] 4. *Comparison*. Comparison of results from the analysis to actual values. This step may involve the use of multiple linear [regression] regressions on 2-4 Principal components to obtain a calibration for different performance indicators.

$$\mathbf{A} = \begin{bmatrix} A_{1,1} & \cdots & A_{1,j} & \cdots & A_{1,p} \\ \vdots & \ddots & \vdots & \ddots & \vdots \\ A_{i,1} & \cdots & A_{i,j} & \cdots & A_{i,p} \\ \vdots & \ddots & \vdots & \ddots & \vdots \\ A_{n,1} & \cdots & A_{n,j} & \cdots & A_{n,p} \end{bmatrix} \quad [1]$$

[0070] In the statistical techniques described by Richardson et al., the sample correlation (r_{ik}) between variables is measured as a function of the variance [(s_{ii})] (s_{jj}) and covariance [(s_{ij})] (s_{jk}) of the data[. In this case i and j] where j and k are two different indexes for the wavelength for the emission (or conversely absorbance) measurement and $[k]$ i is the index for n different samples.

$$r_{jk} = \frac{s_{jk}}{\sqrt{s_{jj}s_{kk}}} \quad [2]$$

$$s_{jj} = s_j^2 = \frac{1}{n-1} \sum_{i=1}^n (A_{i,j} - \bar{A}_j)^2 \quad [3]$$

$$s_{jk} = \frac{1}{n-1} \sum_{i=1}^n (A_{i,k} - \bar{A}_k)(A_{i,j} - \bar{A}_j) \quad [4]$$

$$\mathbf{S} = \begin{bmatrix} s_{11} & s_{12} & \cdots & s_{1p} \\ s_{21} & s_{22} & \cdots & s_{2p} \\ \vdots & \vdots & \ddots & \vdots \\ s_{p1} & s_{p2} & \cdots & s_{pp} \end{bmatrix} \quad [5]$$

$$\mathbf{R} = \begin{bmatrix} 1 & r_{12} & \cdots & r_{1p} \\ r_{21} & 1 & \cdots & r_{2p} \\ \vdots & \vdots & \ddots & \vdots \\ r_{p1} & r_{p2} & \cdots & 1 \end{bmatrix} \quad [6]$$

[0075] (3) Partial Least Squares (PLS) regression is a multivariate data analysis technique that can be used to extract components (now called factors) that relate several response (Y) variables to several explanatory (X) variables. The method aims to identify the underlying factors, or linear combination of the X variables, which best model the Y dependent variables. PLS can deal efficiently with data sets where there are very many variables that are highly correlated and involving substantial random noise.

- c) Richardson et al. in U.S. Patent No. 5,242,602 does not describe the use of PLS although other descriptions of chemometrics describe the power of this technique in chemometric analysis.
- d) However, the partial least squares analysis is no better than the different linear functions that may be described from the data. If the property/characteristic that is to be predicted cannot be described as a linear function of the [variables x] variable X then the regression will introduce systematic error into the regression model.

[0077] Using a set of ratios derived from the original data, the data matrix **A** is transformed into a new [data] matrix that may be called the ratio matrix **[R] Q**. This matrix is based upon a predetermined set of wavenumbers for the numerators and denominators of the ratios. The i index is the index for the sample and the j index is the index for the wavelength of the numerators with a total of j_p numerators that define the set of quotients used, the k index is the index for the set of wavelengths corresponding to the set of denominators that match the j indexed emission (or conversely absorbance) values for each sample. There are a total of k_p index values for the denominators for that define the set of quotients used. The ratio [data] matrix **Q** may be generally written as:

$$Q = \begin{bmatrix} \frac{A_{1,j_1}}{A_{1,k_1}} & \dots & \frac{A_{1,j}}{A_{1,k}} & \dots & \frac{A_{1,j_p}}{A_{1,k_p}} \\ \vdots & \ddots & \vdots & \ddots & \vdots \\ \frac{A_{i,j_1}}{A_{i,k_1}} & \dots & \frac{A_{i,j}}{A_{i,k}} & \dots & \frac{A_{i,j_p}}{A_{i,k_p}} \\ \vdots & \ddots & \vdots & \ddots & \vdots \\ \frac{A_{n,j_1}}{A_{n,k_1}} & \dots & \frac{A_{n,j}}{A_{n,k}} & \dots & \frac{A_{n,j_p}}{A_{n,k_p}} \end{bmatrix} \quad [7]$$

[0077.1] The wavelengths used for the numerators $A_{i,j}$ and the denominators $A_{i,k}$ will be selected from those absorbance or emission wavelengths that yield ratios that correspond well to the component concentration, process or physical property that is to modeled or optimized.

[0081] Principle Component Analysis:

Using 9 UV values, only one factor may be extracted. This factor explains 97.6% of the data variation. There is one other factor with an eigenvalue between 1.0 and [0.1] 0.1.

[0088] 1. The removal of lignin was identified as an important process in the bleaching of pulp. In the prior art this was not thought to be the case for mechanical pulps. However, excessive lignin removal can occur during inefficient bleaching [processes] process that leads to a parallel increase in colored components. The best bleaching occurred when the most lignin could be removed while generating the smallest amount of colored components.

[0092] A plurality of different methods for measuring peroxides [are] is known. Among those, polarigraphic measurements are thought to be unreliable and commercial methods using catalytic peroxide decomposition were not yet available. Presently, a hydrogen peroxide measurement is available from BTG a Division of Spectris Technologies, but the reliability of this measurement is still in question and it has not been widely adapted.

[0096] Figure 9 shows a series of Raman spectra of pressates from peroxide bleaching of pulp. These spectra were obtained using a 1064 nm laser with FT signal processing, baseline correction and subtraction of water spectra. The samples were quantitatively diluted to pH 7

before their measurement. The series progresses from high bleaching pH at the top to low bleaching pH at the bottom. Raman peaks are observed at approximately 530 cm^{-1} for silicate, at approximately 877 cm^{-1} for hydrogen peroxide (H_2O_2), at approximately 990 cm^{-1} for sulfate, and at approximately 1077 cm^{-1} for [and] carbonate. The Raman peaks for sulfate shown in Figure 8 appear due to the addition of sulfate. Sulfate was added in order to lower the pH value. The Raman peaks for carbonate are observed because CO_2 is absorbed from the surrounding atmosphere to form carbonate ions. Alternatively, this method is used for predicting scale formation since it is capable of detecting sulfate ions and carbonate ions. In this case, care is taken that the pressates are not exposed to carbon dioxide.

Table 2

Regression Summary for Dependent Variable: [YIELD] **YIELD**

R= .99912365 R²= .99824807 Adjusted R²= .99562018

F(3,2)=379.87 p<.00263 Std.Error of estimate: .27325

	BETA	St. Err. of BETA	B	St. Err. of B	t(2)	p-level
[Intercept] <u>Intercept</u>			37.37	4.841	7.72089	.016364
RH2O2UV2	.992604	.080541	8322.67	675.313	12.32417	.006520
H2O2	.958102	.091885	32733.36	3139.227	10.42720	.009072
RSILH2O2	.942172	.122940	38.20	4.985	7.66366	.016604

Table 3

Regression Summary for Dependent Variable: H2O2 [residual] **RESIDUAL**

R= .99822460 R²= .99645235 Adjusted R²= .99113086

F(3,2)=187.25 p<.00532 Std.Error of estimate: .11298

	BETA	St. Err. of BETA	B	St. Err. of B	t(2)	p-level
[Intercept] <u>Intercept</u>			-12.085	1.7914	-6.74606	.021275
RH2O2UV2	1.045293	.122605	2546.622	298.7004	8.52567	.013480
RH2O2SIL	1.376609	.171798	1.718	.2144	8.01298	.015220
RSILH2O2	1.395214	.236563	16.437	2.7869	5.89786	.027565

[00100] The ratio formulated between the Raman peak intensity for the peroxide and the silicate is of importance for indicating an optimal stabilizing effect through the silicate. Silicate is added to the bleaching solution to stabilize the peroxide. Thus the amount of silicate with [resoect] respect to hydrogen peroxide is maximized such that it provides best stabilizing effects for the amount of hydrogen peroxide.

Table 4

Start pH	Pulp and Pressate Properties					Raman intensities of pH adjusted pressates			
	Bleach Yield	[H ₂ O ₂] <u>H₂O₂</u> residual	[TDS g/l] <u>TDS</u> g/L	[rightnes ISO] <u>Brightness</u> ISO %	Pulp Bulk	Silicate [530cm ⁻¹] <u>530cm⁻¹</u>	[H ₂ O ₂] <u>H₂O₂</u> 877 cm ⁻¹	SO ₄ [990 cm ⁻¹] <u>980 cm⁻¹</u>	CO ₃ 1077 cm ⁻¹
9.5	97.2	[3.47] <u>3.74</u>	1.17	73.84	3.27	0.25	1.81	1.28	0.96
9.7	96.1	<u>2.38</u>	1.16	74.52	3.17	0.28	1.05	1.27	0.92
10.0	96.0	[2.38]	1.76	77.97	3.12	0.32	1.08	1.29	1.04
10.3	93.6	2.82	1.95	78.93	2.80	0.21	1.06	1.24	0.97
10.5	92.8	1.90	2.21	78.99	2.92	0.20	1.05	1.24	0.96
10.7	93.0	1.89	2.20	79.68	2.38	0.32	0.98	1.34	0.91
11.1	90.2	1.26	2.69	81.82	2.60	0.30	0.98	1.28	0.94
11.5	88.9	0.91	3.15	83.45	2.00	0.40	0.86	1.46	1.01
12.1	86.7	0.04	5.26	80.33	1.69	0.41	0.89	1.38	0.97

[00102] Figure 11 presents Raman Spectra of pressates from hydrogen peroxide bleaching of aspen TMP pulp at different pH values. The spectra are obtained directly, i.e. without dilution or pH adjustment. The Raman peaks for hydrogen peroxide (H₂O₂) at 877 cm⁻¹, for carboxylic acid (COO-) at [924. cm⁻¹], 925 cm⁻¹ for a C-H bending mode at 1350 cm⁻¹, and for a C-H [vending] bending mode at 1415 cm⁻¹ are shown. The relative decrease of the hydrogen peroxide peak and increase in the peaks representing different bleaching by-products can be related to pulp properties developed during bleaching. During the pulp bleaching process with hydrogen peroxide competing chemical processes result in the destruction of colored species, the

cleavage and removal of colored species, and the formation of colored species during non-productive cleavage of lignin substances. Peroxide concentrations decrease during both productive and non-productive reactions through bimolecular degradation of the peroxide or reaction with the wood substances. The spectra in figure 11 and the associated tables 5 and 6 [below,] below show that the productive reactions leading to high brightness with minimal loss of yield and bulk generate carboxylic groups with Raman intensities at [924 cm⁻¹.] 925 cm⁻¹. Smaller amounts of brightness gain and greater yield or bulk loss correlate well with the increase in the intensity of Raman emission peaks at 1350 cm⁻¹ and 1415 cm⁻¹. Hence the greatest improvement in brightness gain with the least [lost] loss of yield or bulk occurs when the amplitude of the intensity ratio of the peak at [924 cm⁻¹] 925 cm⁻¹ to the intensity at 1350 cm⁻¹ or 1415 cm⁻¹ is maximized. The peak intensity for the hydrogen peroxide at 877 cm⁻¹ should be maximized to preserve the hydrogen peroxide and to prevent unnecessary radical reactions. These results provide a basis for improved relationships between the Raman intensities and the pulp properties shown in Tables 7-12. In Table 7 the brightness development is optimized when the relative consumption of the hydrogen peroxide to the development of the C-H peak at [1350 cm⁻¹] 1350 cm⁻¹ is minimized. [In] Table 9 [the] relates the bulk to the product of the peaks at [1350 cm⁻¹] 1350 cm⁻¹ and [1415 cm⁻¹] 1415 cm⁻¹, as formation of compounds contributing to [these] both of these peaks [contribute] contributes to brightness loss.

Table 5

pH		ISO % [brightness] <u>Brightness</u>	[freeness] <u>Freeness</u>	[bulk] <u>Bulk</u>	[H ₂ O ₂] <u>H₂O₂% in</u> pressate	% on pulp	TOC	[yield] Yield
initial	final							
9.3	6.4	72.17	164.5	2.931	0.577	[2.974] <u>2.942</u>	1580	98.102
9.6	6.5	72.56	149.0	2.967	0.548	2.825	1550	98.138
10.0	7.1	74.49	148.0	2.901	0.359	1.850	3030	96.361
10.2	7.3	75.17	143.0	2.774	0.311	1.604	3610	95.664
10.5	7.4	76.05	147.0	2.750	0.277	1.428	4070	95.112
10.7	7.6	76.03	152.0	2.815	0.245	1.262	4570	94.511
11.0	8.0	77.58	142.0	2.620	0.147	0.760	6550	92.133
11.4	8.4	78.32	132.0	2.453	0.088	0.451	6400	92.313
11.8	9.0	78.25	129.0	1.954	0.075	0.388	[13100] <u>13000</u>	84.266

Table 6

pH		UV [ABS] <u>Abs 280 nm</u>	Raman Intensities			
initial	final		[I_876] <u>I₈₇₇</u>	[I_1924] <u>I₉₂₅</u>	[I_1350] <u>I₁₃₅₀</u>	[I_1415] <u>I₁₄₁₅</u>
9.3	6.4	0.588	1.960	0.532	0.364	0.496
9.6	6.5	0.578	1.585	0.434	0.263	0.409
10.0	7.1	[0860] <u>0.860</u>	1.207	0.799	[0334] <u>0.344</u>	0.666
10.2	7.3	1.013	0.996	0.893	0.441	0.653
10.5	7.4	1.183	0.888	0.964	0.469	0.797
10.7	7.6	1.269	0.797	0.971	0.471	0.795
11.0	8.0	2.164	0.656	1.559	0.731	1.181
11.4	8.4	3.193	0.324	1.647	0.877	1.334
11.8	9.0	4.371	0.587	1.782	1.216	1.750

Table 8

Regression Summary for Dependent Variable: **BULK**
 $R = .98249292$ $R^2 = .96529234$ Adjusted $R^2 = .96033411$
 $F(1,7) = 194.68$ $p < .00000$ Std.Error of estimate: .06333

	BETA	St. Err. of BETA	B	St. Err. of B	t(7)	p-level
[Intercept] <u>Intercept</u>			3.264	.04657	70.0903	.000000
I1350	-.982493	.070415	-521.783	37.39594	-13.9529	.000002

Table 9

The Ratio Predicts bulk better

Regression Summary for Dependent Variable: **BULK**
 $R = .99113735$ $R^2 = .98235324$ Adjusted $R^2 = .97983227$
 $F(1,7) = 389.67$ $p < .00000$ Std.Error of estimate: .04516

	BETA	St. Err. of BETA	B	St. Err. of B	t(7)	p-level
[Intercept] <u>Intercept</u>			3.	.022	138.9712	.000000
[P1350141] <u>P13501415</u>	-.991137	.050209	-127757.	6471.954	-19.7401	.000000

Table 10

Regression Summary for Dependent Variable: **H2O2 residual on Pulp**
 $R = .99806738$ $R^2 = .99613850$ Adjusted $R^2 = .99382159$
 $F(3,5) = 429.94$ $p < .00000$ Std.Error of estimate: .07356

	BETA	St. Err. of BETA	B	St. Err. of B	t(5)	p-level
[Intercept] <u>Intercept</u>			.799	.16514	4.84114	.004710
R8761350	.360850	.103708	.163	.04689	3.47948	.017669
I1415	-.252501	.050347	-279.289	55.68855	-5.01519	.004052
1876	.427770	.094706	403.384	89.30762	4.51680	.006301

Table 11

Regression Summary for Dependent Variable: **TOC**
 R= .96431621 R²= .92990576 Adjusted R²= .91989230
 F(1,7)=92.866 p<.00003 Std.Error of estimate: 1002.7

	BETA	St. Err. of BETA	B	St. Err. of B	t(7)	p-level
[Intercept] <u>Intercept</u>			-1394.	737.4	-1.89022	.100643
I1350	.964316	.100067	5705570.	592068.1	9.63668	.000027

Table 12

Regression Summary for Dependent Variable: **TOC**
 R= .99132396 R²= .98272319 Adjusted R²= .97235711
 F(3,5)=94.802 p<.00008 Std.Error of estimate: 589.00

	BETA	St. Err. of BETA	B	St. Err. of B	t(5)	p-level
Intercept			-1989.	1509.	-1.31791	.244683
Product I1350•I1415	2.031475	.447598	29173073E2	642774566.	4.53862	.006177
Ratio I924/I1350	.208308	.072085	2406.	832.	2.88976	.034197
UV280 [abs] <u>Abs</u>	-.993688	.435777	-2691.	1180.	-2.28027	.071514

[00106] [Figure 14 shows] Figures 14A to 14J show a matrix plot of Raman intensities and Raman ratios as a function of pH. The considered Raman intensities are the Raman intensities for hydrogen peroxide HOOH (I877) and peroxy ions HOO⁻ (I850) as a function of pH. Two ratios of Raman peak intensities are also shown in the matrix plot. The Raman intensity ratio of R850877 is the intensity of the peak at 850 cm⁻¹ to the intensity of the peak at 877 cm⁻¹, the Raman intensity ratio R877T is the [ration] ratio of the 877 cm⁻¹ peak to the sum of the two peak intensities at 850 cm⁻¹ and 877 cm⁻¹. These intensity ratios give new non-linear variables that relate to the peroxide solutions properties. The matrix plot shows the relationship between the [brightness] solution pH and the Raman peak intensities of the HOO⁻ and HOOH peroxide species. The use of these peak intensities for the measurement and control of hydrogen peroxide concentrations in pulp and paper and water treatment has not been described. Thus in accordance with an embodiment of the present invention the Raman peak intensities of the

Raman peaks at 850 cm^{-1} and 877 cm^{-1} are used to control the hydrogen peroxide concentration. The ratio of the peak intensities provides a new relationship with respect to the solution properties (pH) as shown in plot 14C. The ratio is different than the direct peak intensities as shown in Figures 14F and 14H. Raman peak intensity ratios or products provide [different] alternative means by which the properties [are modeled] can be modeled. A [by influencing variables.A] second ratio may be defined by the intensity of one peak to the sum of the intensity of both Raman peaks. This ratio is expected to follow relationships relevant to the pKa of the peroxide. Figures 14F and 14H show nonlinear relationships between the ratio and the direct peak intensity thus confirming that [[00107] The] the matrix plot presented in Figure 14 does not show a product of the intensities of the two Raman peak intensities at 850 cm^{-1} and 877 cm^{-1} . However, the product of these two Raman peak intensities provides similar results as the ratio between two Raman peak intensities.

[00108] [The Measurement of the Redox Properties and Relative Concentrations of Related Oxidative and Reductive Species] The Measurement of the Redox Properties and Relative Concentrations of Related Oxidative and Reductive Species

[00110] Figure 17 presents spectra showing Raman intensities of a solution of sodium hydrosulfite ($\text{Na}_2\text{S}_2\text{O}_4$) oxidizing to sulfate and sulfite ions. The management of oxidizing and reducing substances in industrial applications is problematic in part because measures such as an [oxidation reduction] oxidation-reduction potential (ORP) are very sensitive to pH, ionic strength, temperature and the influence of interfering substances. The use of Raman peak intensities provides a means to directly measure the concentrations and relative concentrations of the different species contributing to the oxidation potential of the solution.

[00112] Figure 19 presents a matrix plot showing Raman intensities, and Raman intensity [oxidation reduction] oxidation-reduction potential (ORP). Regression lines plot of Figure 19 demonstrate that the Raman intensity ratios correlate than their components. Plots *P* and *R* within Figure 19 demonstrate that a provides the best direct measure of the ORP of the sulfur species in plots are almost linear.

[00113] Table 13 provides a regression summary for the [oxidation reduction] oxidation-reduction potential and Table 14 shows the correlations for hydrosulfite oxidation.

Table 13

Regression Summary for Dependent Variable: ORP
 $R = .99514836$ $R^2 = .99032025$ Adjusted $R^2 = .98709366$
 $F(1,3) = 306.93$ $p < .00041$ Std.Error of estimate: 6.0576

	BETA	St. Err. of BETA	B	St. Err. of B	t(3)	p-level
Intercept			-206.467	9.147723	-22.5703	.000190
Ratio I460/[I977] I980	-.995148	.056803	-75.062	4.284508	-17.5193	.000405

ORP = $-206.467 - 75.062 * \text{I460} / [\text{I977}] \text{ I980}$

Table 14**Correlations Hydrosulfite Oxidation**[Marked correlations are significant at $p < .05000$]

	[time] Time	ORP	I228	I460	I583	[I980] I977	I998	I1022	Ratio 583/ [977] 980	Ratio [977] 980/ 998	Ratio 460/ [977] 980	Ratio [977] 980/ 1022
TIME	1.00	.94	-1.00	-.99	-1.00	.94	-1.0	-.79	-.94	.90	-.94	.90
ORP	.94	1.00	-.98	-.99	-.95	.97	-.88	-.96	-.99	.93	-1.00	.96
I228	-1.00	-.98	1.00	1.00	1.00	-.94	.99	.79	.94	-.91	.94	-.90
I460	-.99	-.99	1.00	1.00	1.00	-.94	.99	.79	.96	-.89	.96	-.89
I583	-1.00	-.95	1.00	1.00	1.00	-.94	1.0	.79	.96	-.89	.95	-.89
[I980] I977	.94	.97	-.94	-.94	-.94	1.00	-.95	-.93	-.87	.98	-.87	.99
I998	-1.00	-.88	.99	.99	1.00	-.95	1.0	.81	.95	-.91	.94	-.91
I1022	-.79	-.96	.79	.79	.79	-.93	.81	1.00	.75	-.91	.76	-.96
Ratio 583/[977] 980	-.94	-.99	.94	.96	.96	-.87	.95	.75	1.00	-.77	1.00	-.81
Ratio [977] 980/998	.90	.93	-.91	-.89	-.89	.98	-.91	-.91	-.77	1.00	-.77	.99
Ratio 460/[977] 980	-.94	-1.00	.94	.96	.95	-.87	.94	.76	1.00	-.77	1.00	-.80
Ratio [977] 980/1022	.90	.96	-.90	-.89	-.89	.99	-.91	-.96	-.81	.99	-.80	1.00

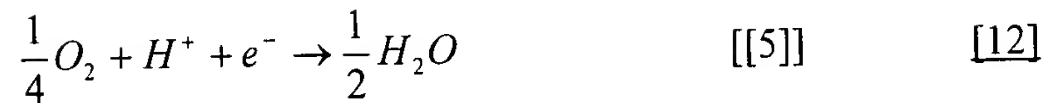
[00114] The [Oxidation/Reduction Potential] oxidation-reduction potential (ORP) is a measurement of the potential for a reaction to occur. [Oxidation-Reduction] Oxidation-reduction represents electron concentration and activity level. An ORP in the plus range indicates oxidation, i.e. the absence of energy, and an inability to perform additional chemical reactions. An ORP in the negative range indicates chemical reduction, i.e. the presence of electrons, potential energy, and the ability to generate additional chemical reactions. ORP is therefore a measure of energy potential. The more negative the ORP, the more electrons present (in relation to the number of protons), and the more energy available. Biological redox reactions are a result of hydrogen being the essential electron donor, and oxygen being the essential electron acceptor.

$$pE = pE^- + \frac{1}{n} \log_{10} \frac{\{A_{ox}\}}{\{A_{red}\}} \quad [[1]] \quad [8]$$



$$pE = pE^- + \log_{10} \frac{\{H^+\}}{f_{H_2}^{\frac{1}{2}}} \quad [[3]] \quad [10]$$

$$pE = -pH \quad [[4]] \quad [11]$$



$$pE = pE^- + \log_{10} [f_{O_2}^{\frac{1}{2}}] \underline{f_{O_2}^{\frac{1}{4}}} \{H^+\} \quad [[6]] \quad [13]$$

$$pE = 20.75 - pH \quad [[7]] \quad [14]$$

[00125] The pE for natural waters can be calculated using equation [[6]] [13]. The unknowns which must be measured are pH and the O2 partial pressure (concentration). For example, the pE for surface water in equilibrium with the atmosphere ($p_{O_2} = 0.21$ atm) and have a pH of 8 would be:

$$pE = pE^- + \log_{10} f_{O_2}^{\frac{1}{4}} \{H^+\} \quad [[8]] \quad [13]$$

$$pE = pE^- - pH + \log_{10} [f_{O_2}^{\frac{1}{2}}] \underline{f_{O_2}^{\frac{1}{4}}} \quad [[9]] \quad [15]$$

$$pE = 20.75 - 8 + \log_{10} (0.21)^{\frac{1}{4}} = 12.58 \quad [[10]] \quad [16]$$

$$pE = 20.75 - pH \quad [[11]] \quad [14]$$

$$pE = -pH \quad [[12]] \quad [11]$$

[00129] Figure 21 shows the intensities of the different peaks as derived from the spectra presented in Figure 20. Figure 21 shows a matrix plot of Raman intensities as a function of the $[HO^-/Si]$ NaOH/Si ratio as derived from Prabir K. Dutta and Dah-Chung Shieh, *Applied Spectroscopy*, Vol. 39, No. 2, 343-346 (1985). Peaks from silicate relate to different vibrational modes that depend on the ionization and degree of polymerization of the silicate. Vibrations from silicate monomers yield peaks at 925 cm^{-1} (Si-O⁻ stretch, monomer ionized) 772 cm^{-1} (Si-O-H stretch, monomer not ionized), 482 cm^{-1} (Si-OH stretch) and 446 cm^{-1} (SiO₂(OH)₂²⁻ symmetric bend). Dimer groups yield peaks at 598 cm^{-1} (Si-O-Si stretch, dimer bridge) and 1014 cm^{-1} (SiO₃ stretch, dimer endgroup). Cyclic trimers have a breathing vibration at 531 cm^{-1} . The peak at 1014 cm^{-1} (SiO₃ stretch, dimer endgroup) shifts to $\sim 1030\text{ cm}^{-1}$ with cyclic trimers.

[00131] Ratios present the physical properties of the silicates better than intensities alone do. This is demonstrated in Figure 22 showing a matrix plot of Raman intensity ratios as a function of the HO⁻/Si ratio from Prabir K. Dutta and Dah-Chung Shieh, *Applied Spectroscopy*, Vol. 39, No. 2, 343-346 (1985). It is noted that this article does not teach the use of ratios. The intensities given in this article were used to derive Raman intensity ratios in order to demonstrate that the use of Raman intensity ratios is much better in predicting the physical properties of silicates. The ratios relate the relative concentrations of different functional groups characterizing the silicate speciation. These ratios provide new variables that logically relate to the properties of the silicate solution. The ratio $[R_{579/1014}]$ R_{597/1014} is related to the degree of polymerization or the chain length because individual intensities represent the amount of bridging/the amount of end groups, i.e. ratio of the peak intensity at 597 cm^{-1} to the intensity at 1014 cm^{-1} . The degree of polymerization decreases with increasing alkali concentration. The ratio $R_{925/772}$ is related to the degree of amount of ionization of the silicate monomers (ratio of the peak intensity at 925 cm^{-1} to the intensity at 772 cm^{-1}). The ratio $R_{531/597}$ is related to the ratio of cyclic trimer groups to dimer groups (ratio of the peak intensity at 531 cm^{-1} to the

intensity at 597 cm^{-1}). The ratio $R_{531/772}$ is related to the ratio of cyclic trimer groups to protonated monomer groups (ratio of the peak intensity at 531 cm^{-1} to the intensity at 772 cm^{-1}). The ratio $R_{531/925}$ is related to the ratio of cyclic trimer groups to ionized monomer groups (ratio of the peak intensity at 531 cm^{-1} to the intensity at 925 cm^{-1}). The ratio $R_{1014/925}$ is related to the ratio of ionized dimer groups to ionized monomer groups (ratio of the peak intensity at 1014 cm^{-1} to the intensity at 925 cm^{-1}).

Example of The Use of Raman Spectra and Ratios for Measurement and Control of Pulp Bleaching[.]

[00134] There are 10 different samples (PH = 9.5, 9.7, 10.0, 10.3, 10.5, 10.7 11.5, 11.7, 12.1 and 12.7). Since each sample [adjust] adjusts the final pH by using buffer solution (pH = 6.9) and 1M NaOH, these 10 [sample] samples have been divided into two groups. There is one group with three peaks at 877, [990] 980 and 1077 cm^{-1} , and another group having two broad bands at 1100 and 1630 cm^{-1} . These two broad bands are due to water and the Raman sample cell. As described above, water was subtracted from the obtained Raman spectra before processing the data.

[00135] According to the reference Raman spectra of H_2O_2 , the peak at 877 cm^{-1} in bleaching water is due to the H_2O_2 . The amount of the H_2O_2 is approximately 0.1%. The peak at [990 cm^{-1}] 980 cm^{-1} is due to SO_4 stretching band of the sulfate (reference see previous work). The amount of H_2O_2 decreases with the pH increase, while the amount of the sulfate increases with the pH increase. The detection limit for H_2O_2 and SO_4 can be lowered down to 0.1% at current instrument condition. Interfering peaks due to carboxylic acid vibrations occur at 890 cm^{-1} for acetic acid and [927 cm^{-1}] 925 cm^{-1} for the acetate ion.

Other Examples of Raman Spectra of Ultrafiltered Pulp Processing Waters

[00137] Raman spectra of two white water samples from Millar Western Pulp (MWP) and one from Alberta Newsprint (ANC) are collected and shown in Figure 23. These samples are filtered through a [0.45 micron] 0.45 μ filter before data is collected. Only one band at [990 cm^{-1}] 980 cm^{-1} appears in ANC water. It is the contribution of the SO_4 (sulfate ion) band from the sulfate. There are also some sulfates in two kinds of Millar Western Pulp water. The

amount of sulfate is different according to the band intensities. The peak at 877 cm^{-1} in both Millar Western Pulp water samples also indicates the existence of H_2O_2 . Another band at 925 cm^{-1} in two MWP water samples is [possibly] the contribution of the acetate [buffer solution] carboxylate groups in the water. Figure 24 gives the Raman [and IR] spectra of acetic acid and acetic buffer acetate solution (0.05M). [The amounts of the buffer solution are different in these two kinds of different water samples.] The peak at 925 cm^{-1} is due to $\nu\text{C-O}$ of the carboxylic group (basic form), the peak at 890 cm^{-1} is due to the same vibration mode but from the acid form.

[00138] Other relevant small molecules and complex ions in the pulp and paper industry may be detected. These species include SO_4^{2-} , $\text{S}_2\text{O}_3^{2-}$, SO_3^{2-} , H_2O_2 , ClO_2 , HClO_3 , silicates, acetic acid, Chloric Acid HClO_3 , Chlorate $\text{ClO}_3(-)$, Chlorous Acid HClO_2 , Chlorite $\text{ClO}_2(-)$, Hypochlorous Acid HClO , Hypochlorite $\text{ClO}(-)$, phosphate, nitrate, nitrites.

In the Claims:

6. A method as defined in claim 2 wherein the Raman intensity for peroxide is obtained at approximately $[875\text{ cm}^{-1}]$ 877 cm^{-1} and the Raman intensity for the peroxy ion is obtained at approximately 850 cm^{-1} .

13. A method as defined in claim 12 wherein the non-linear relationship is expressed as at least one of the following functions between the property of the sample and the first and second measurement:

property of sample = $f(\text{first measurement, first measurement} / \text{second measurement})$;

property of sample = $f(\text{first measurement, first measurement} * \text{second measurement})$;

property of sample = $f(\text{first measurement, first measurement} / (\text{first measurement} + \text{second measurement}))$; and

property of sample = $f(\text{first measurement, } (\text{first measurement} + \text{second measurement}) / \text{first measurement})$.

25. A method as defined in claim 18 wherein the property is an oxidation-reduction potential of the sample or another measure of the oxidative or reductive capacity of the sample.

33. A method as defined in claim 31 wherein the molecules include sulfides, cyanides, chromates, [and] nitrates and carbonates.

38. An apparatus as defined in claim 37 wherein the non-linear relationship is expressed as at least one of the following functions between the property of the sample and the first and second measurement:

property of sample = $f(\text{first measurement}, \text{first measurement} / \text{second measurement})$;

property of sample = $f(\text{first measurement}, \text{first measurement} * \text{second measurement})$;

property of sample = $f(\text{first measurement}, \text{first measurement} / (\text{first measurement} + \text{second measurement}))$; and

property of sample = $f(\text{first measurement}, (\text{first measurement} + \text{second measurement} / \text{first measurement}))$.